Large-scale glaciation and deglaciation of Antarctica during the Late Eocene

Shanan E. Peters[1], Anders E. Carlson[1], Daniel C. Kelly[1], and Philip D. Gingerich[2]
[1]Department of Geoscience, University of Wisconsin, Madison, Wisconsin 53706, USA
[2]Department of Geological Sciences and Museum of Paleontology, University of Michigan, Ann Arbor, Michigan 48109, USA

ABSTRACT

Approximately 34 m.y. ago, Earth's climate transitioned from a relatively warm, ice-free world to one characterized by cooler climates and a large, permanent Antarctic Ice Sheet. Understanding this major climate transition is important, but determining its causes has been complicated by uncertainties in the basic patterns of global temperature and ice volume change. Here we use an unusually well exposed coastal incised river-valley complex in the Western Desert of Egypt to show that eustatic sea level fell and then rose by ~40 m 2 m.y. prior to establishment of a permanent Antarctic Ice Sheet. This fall in sea level is associated with a positive oxygen isotope excursion that has been interpreted to reflect global cooling, but instead records buildup of an Antarctic Ice Sheet with a volume ~70% of the present-day East Antarctic Ice Sheet. Both the sea-level fall and subsequent rise were coincident with a transient oscillation in atmospheric CO_2 concentration down to ~750 ppm, which climate models indicate may be a threshold for Southern Hemisphere glaciation. Because many of the carbon emission scenarios for the coming century predict that atmospheric CO_2 will rise above this same 750 ppm threshold, our results suggest that global climate could transition to a state like the Late Eocene, when a large permanent Antarctic Ice Sheet was not sustainable.

INTRODUCTION

Earth's climate has undergone numerous transitions between globally warm periods, with warm temperate conditions extending nearly to the poles, and globally cool periods, when large continental ice sheets formed and extended to middle latitudes (Zachos et al., 2008). The greatest global shift to cooler climate in the Cenozoic occurred near the Eocene-Oligocene boundary, ca. 33.8 Ma. Cooling and growth of continental ice during this time are evidenced by a large positive excursion in the mean $\delta^{18}O$ composition of benthic and planktonic foraminifera (Kennett, 1977; Miller et al., 1987; Zachos et al., 2001; Katz et al., 2008), deepening of the ocean's calcite compensation depth (Rea and Lyle, 2005; Coxall et al., 2005), a decline in high-latitude sea surface temperatures (Liu et al., 2009), and widespread deposition of ice-rafted debris and glacial till at high southern latitudes (Wilson et al., 1998). Proposed mechanisms for this fundamental change in the global climate system include a decrease in atmospheric CO_2 (DeConto and Pollard, 2003; Huber and Nof, 2006; Pearson et al., 2009), a minimum in solar insolation (Coxall et al., 2005), and changes in ocean circulation caused by the opening of the Southern Ocean and isolation of the Antarctic continent (Kennett, 1977).

Despite ample evidence for global cooling and expansion of the Antarctic Ice Sheet near the Eocene-Oligocene boundary (Barker et al., 2007; Lear et al., 2008), the magnitudes of global temperature and ice volume changes during the Late Eocene remain poorly constrained. This is primarily because one of the most widely used indicators of paleoclimate, the $\delta^{18}O$ composition of marine carbonates, cannot distinguish between changes in temperature and changes in continental ice volume. Uncertainty about the relative contributions of these two factors is particularly acute for initial phases of the Eocene-Oligocene climate transition, when temperature and ice volume fluctuations may have been transient, decoupled, and below the detection limits of temperature proxy records (Zachos et al., 2001, 2008; Liu et al., 2009).

Here we provide new constraints on the magnitude of Late Eocene glacioeustatic sea-level fluctuations by studying an unusually well exposed coastal incised valley fill complex at Wadi Al-Hitan in the Western Desert of Egypt (Fig. 1). Incised valley fills are formed by fluvial erosion and downcutting during a fall in sediment base level, which in coastal regions is controlled principally by lowering of sea level (Zaitlin et al., 1994). Subsequent rise in sea level traps fluvial and estuarine sediment in the newly cut river valley, thereby forming an incised valley fill. Evidence for Late Eocene sea-level change has been found globally (e.g., Hardenbol et al., 1998; Barker et al., 2007; Katz et al., 2008; Miller et al., 2008). However, the sections at Wadi Al-Hitan provide a unique opportunity to rigorously quantify the magnitude of sea-level fluctuation during this critical period of Earth history, because they are among the best exposed Late Eocene marine coastal sections in the world.

METHODS

At Wadi Al-Hitan, it is possible to trace a coastal incised valley fill complex and its adjacent interfluve over a distance of >16 km nearly parallel to an ancient shoreface (Fig. 1). Sediments within the incised valley fill preserve unambiguous indicators of deposition in fluvial and estuarine environments, including asymmetric current ripples with unimodal transport vectors, lags of imbricated pebbles containing whale fossils that were reworked from underlying marine sediments and mixed with remains of terrestrial mammals, and tidal rhythmites that contain dicot plant leaves but no marine

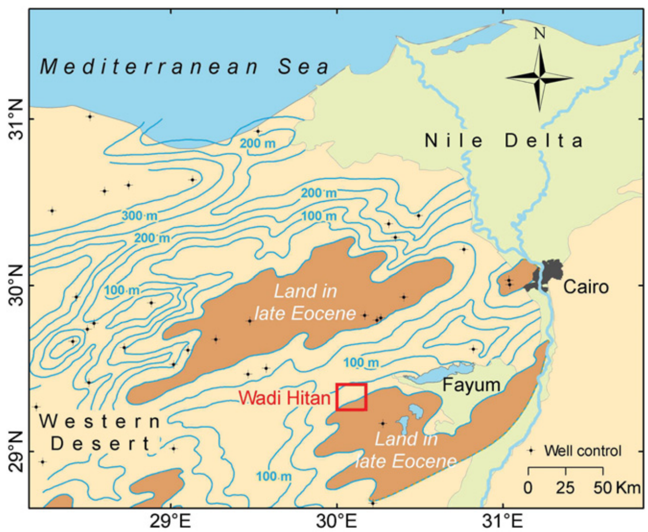

Figure 1. Map showing Wadi Hitan (red rectangle) in context of modern geography and Late Eocene paleogeography. Blue contours show Late Eocene sediment thickness in subsurface oil well sections (Salem, 1976). Black crosses show oil well sections.

Geology, August 2010; v. 38; no. 8; p. 723–726; doi: 10.1130/G31068.1; 3 figures; Data Repository item 2010198.

fossils (Peters et al., 2009). The intensively bioturbated, fossil-bearing marine sandstones into which the incised valley fill is cut were deposited in environments that range from transition zone to shoreface (Peters et al., 2009; see the GSA Data Repository[1]).

Upstream parameters, such as drainage area, precipitation patterns, and bedrock characteristics, influence large-scale incised valley fill geometry, particularly cross-sectional area (Mattheus et al., 2007); however, the maximum incision depth of coastal incised valley fill complexes is controlled primarily by the magnitude and rate of sediment base-level fall (Zaitlin et al., 1994). In coastal environments, base level, or the point at which down-elevation sediment transport potential approaches zero, is controlled principally by sea level, with smaller contributions from the depth and intensity of wave agitation. In order for an incised valley fill to be preserved in the rock record, subsequent rise in base level must trap fluvial and estuarine sediment within the river valley, thereby filling the valley and restoring a planar geomorphic surface. Coastal incised valley fills, therefore, provide important constraints on the magnitude of sea-level fall as well as evidence for subsequent sea-level rise.

Our mapping of the 7 km incised valley fill extent shows that the valley floor varies considerably in depth, but has a maximum incision of 46 m (Fig. 2). To convert the observed maximum incised valley fill incision depth to a minimum estimate of eustatic sea-level fall, it is first necessary to adjust for isostatic rebound of the crust that may occur when the gravitational load imposed by seawater is removed. Assuming an instantaneous isostatic regional adjustment for ~10–20 m of seawater removal prior to fluvial incision, a conservative estimate for the global minimum sea-level fall required to form a 46-m-deep coastal incised valley fill complex is 42 ± 1 m (see the Data Repository). Although it is necessary to account for the gravitational effects of ice-mass distribution on sea surface elevation, this geoid effect is expected to account for only 1–2 m of sea-level change in the southeastern Mediterranean region (Mitrovica et al., 2009; see the Data Repository). Thus, the estimated minimum eustatic sea-level fall required to form the incised valley fill is 40 ± 2 m.

The entire incised valley fill succession is capped by fossiliferous marine sediments that record a subsequent rise in sea level that was of sufficient magnitude and rapidity to overcome fluvial sediment supply and fill the incised valley fill with estuarine sediment, to displace the shoreface landward, and to restore shallow-marine (~10 m) conditions to the region. Thus, the rise in sea level recorded by the incised valley fill succession is comparable in magnitude to that of the preceding fall (~40 m). An additional ~90 m of Late Eocene marine sediment was deposited above the incised valley fill prior to the Eocene-Oligocene boundary (see the Data Repository).

Because the incised valley fill at Wadi Al-Hitan is exceptionally well exposed, it is possible to trace stratigraphic surfaces continuously within and adjacent to the incised valley fill. Doing so revealed the erosional remnants of shorter duration sequences that formed during multiple cycles of subaerial exposure and fluvial incision followed by marine inundation and incised valley fill formation. The rapidity and cyclical nature of the ~10–15 m sea-level changes that are evidenced by these smaller scale sequences are inconsistent with control of local sea level by faulting or other vertical crustal motion (Watts, 1982). Instead, the stratigraphic data indicate rapid eustatic sea-level changes superimposed on a longer term and larger magnitude eustatic sea-level fall and rise.

Additional support for the hypothesis that eustatic sea-level changes were responsible for the formation of the incised valley fill complex at Wadi Al-Hitan derives from sequence stratigraphic analyses conducted in other regions. The marine sediments that enclose the incised valley fill yield age-diagnostic calcareous nannoplankton, and some of the recovered taxa have overlapping global first and last appearance datums that constrain the age of the incised valley fill (see the Data Repository). In particular, the presence of *Isthmolithus recurvus* Deflandre and *Neococcolithes minutus* (Perch-Nielsen) constrains the timing of incised valley fill formation to near the base of nannofossil Zone NP19-20 (Perch-Nielsen, 1989), ca. 36 Ma (Berggren et al., 1995; Gradstein et al., 2004). Thus, the sequence boundary that floors the incised valley fill is equivalent to the Pr-2 sequence boundary at the base of NP19-20 in Europe (Hardenbol et al., 1998) and the American Gulf Coast (Miller et al., 2008). Evidence for a significant sea-level fall and rise near the transition between Zones NP18 and NP19-20 is, therefore, not limited to

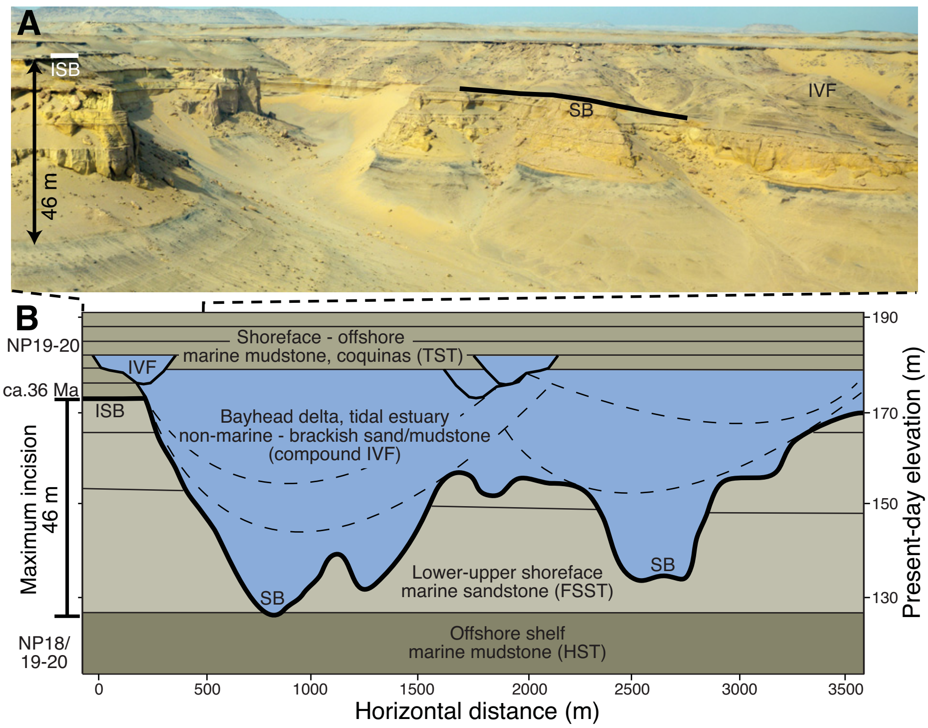

Figure 2. Field image and schematic cross section of incised valley fill (IVF) and enclosing marine sediments. A: Panoramic overview of IVF margin. Dashed lines show lateral position of photo in B. B: Schematic cross section based on digital field mapping (see footnote 1). Subhorizontal thin black lines show traceable marine stratigraphic surfaces. Heavier black lines are sequence boundaries (SB). Heaviest line marks main SB at base of IVF complex. Subsidiary SBs are shown by thinner bold lines. Dashed lines represent unmapped SBs within IVF complex. Note truncation of subhorizontal marine strata by IVF. Minimum sea-level fall is estimated from vertical distance that separates interfluve SB (ISB) from SB at deepest point of IVF (maximum incision). Vertical exaggeration ~22×. TST—transgressive systems tract; FSST—falling stage systems tract; HST—highstand systems tract

[1]GSA Data Repository item 2010198, supplemental materials, methods, and figures, is available online at www.geosociety.org/pubs/ft2010.htm, or on request from editing@geosociety.org or Documents Secretary, GSA, P.O. Box 9140, Boulder, CO 80301, USA.

Egypt. However, because the section at Egypt is exceptionally well exposed and preserves unambiguous and laterally traceable incised valley fill deposits, it is possible to measure the magnitude of sea-level fluctuations in ways that are not possible elsewhere.

DISCUSSION

Biostratigraphic data indicate that the timing of valley incision closely coincides with a +0.30‰ shift in mean benthic $\delta^{18}O$ (Figs. 3A and 3D; see the Data Repository). This positive excursion has previously been assumed to record 1–2 °C of cooling precursory to glaciation in Antarctica (Vonhof et al., 2000). Given, however, that the formation of the Egyptian incised valley fill complex requires substantial eustatic sea-level fall and rise within a geologically short time interval, the positive $\delta^{18}O$ excursion is more likely to be the isotopic expression of continental ice-sheet growth. Because CO_2 levels in the Late Eocene were above the threshold for Northern Hemisphere glaciation (Pagani et al., 2005; DeConto et al., 2008), the most probable locus of such growth is Antarctica.

With a new independent estimate for the magnitude of glacioeustatic sea-level change, it is possible to predict the $\delta^{18}O$ excursion that would be expected due only to ice volume effects. Climate model simulations from the Eocene-Oligocene transition indicate a mean Antarctic ice $\delta^{18}O$ composition of −30‰ ± 5‰ (DeConto et al., 2008). The growth of a 40 ± 2 m sea-level–equivalent volume of this ice would increase the mean $\delta^{18}O$ of ocean water by 0.34‰ ± 0.07‰ (see the Data Repository). Thus, it is likely that most or all of the observed +0.30‰ $\delta^{18}O$ shift ca. 36.0 Ma was caused by an increase in continental ice volume rather than 1–2 °C cooling of the deep ocean (Vonhof et al., 2000). High-latitude sea surface temperature records also suggest reduced amounts of cooling relative to previous estimates, although uncertainties and low sample resolution preclude precise temperature estimates for this event (Liu et al., 2009).

The positive $\delta^{18}O$ excursion ca. 36.0 Ma is followed by a negative excursion of similar magnitude ca. 35.8 Ma (Fig. 3D). This decrease in $\delta^{18}O$ reflects the retreat of ice on Antarctica and is recorded stratigraphically at Wadi Al-Hitan by the in-filling of the incised valley fill with fluvioestuarine sediment and by the restoration of shallow, normal marine shelf conditions to the region (Fig. 2). Numerous cycles of ~10 m sea-level rise and fall within the incised valley fill and in the immediately overlying marine strata indicate increased volatility in sea level during periods of large-scale Antarctic glaciation (see the Data Repository), possibly in response to orbital forcing of ice growth and decay. Changes of ~10 m in sea-level–equivalent volumes of ice would affect benthic $\delta^{18}O$ by only ~0.08‰, which is below the detection level of global mean benthic $\delta^{18}O$ records (Fig. 3D).

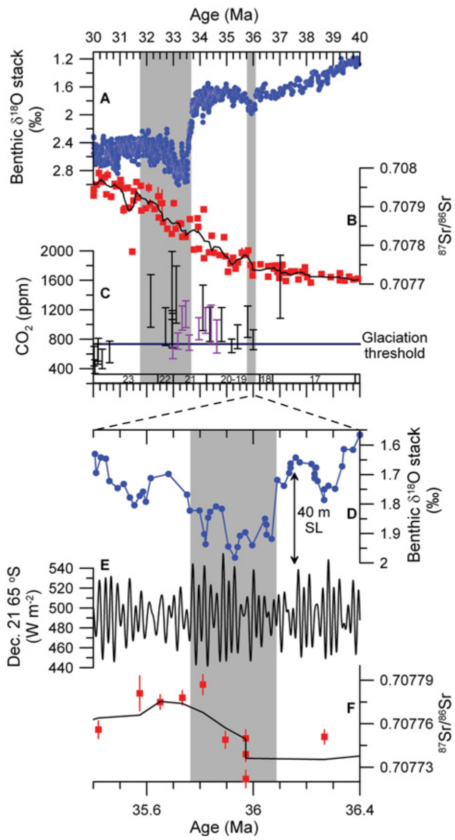

Figure 3. Oxygen and strontium isotopes, CO_2, and insolation during Eocene-Oligocene (E-O) climate transition. A: Global benthic $\delta^{18}O$ stack with 5-point smoothing (Zachos et al., 2001, 2008). The +0.30‰ excursion ca. 36 Ma (gray bar) is observed in individual benthic records (Vonhof et al., 2000; Zachos et al., 1999; Ehrmann and Mackensen, 1992). B: Foraminifera $^{87}Sr/^{86}Sr$ from Ocean Drilling Program (ODP) Site 689B (Mead and Hodell, 1995); red symbols—individual measurements, black line—5-point smoothing. Lower-resolution $^{87}Sr/^{86}Sr$ records from ODP Sites 744 and 748 are similar (Zachos et al., 1999). C: Atmospheric CO_2; black bars are from Pagani et al. (2005), purple bars are from Pearson et al. (2009). Horizontal blue line indicates Antarctic glaciation CO_2 threshold of 750 ppm (DeConto and Pollard, 2003; DeConto et al., 2008). Gray bars denote ~0.3‰ $\delta^{18}O$ increase and larger $\delta^{18}O$ increase at E-O boundary. Calcareous nannoplankton zones (NP17–NP23) are shown on x axis (Gradstein et al., 2004). D: Benthic $\delta^{18}O$ stack. Vertical range shows 40 m eustatic sea-level (SL) component of the $\delta^{18}O$ increase as determined from incised valley fill (IVF). E: 21 December insolation at 65 °S (Laskar et al., 2004). F: Foraminifera $^{87}Sr/^{86}Sr$ (Mead and Hodell, 1995). Gray bar shows interval of ~0.3‰ $\delta^{18}O$ increase.

Agreement between the new physical stratigraphic evidence for sea-level fall and the well-known benthic $\delta^{18}O$ excursion is compelling, and substantial glaciation of Antarctica in the Late Eocene predicts other evidence for ice-sheet advance and retreat. For example, continental glaciation leads to enhanced physical erosion of bedrock and to increased chemical weathering during periods of ice retreat (Blum and Erel, 1995). Because East Antarctica, the locus of ice growth (DeConto and Pollard, 2003), is predominately composed of granitic terrains (Roy et al., 2007), large-scale glaciation during the Late Eocene should have caused an increase in the Sr isotopic composition of ocean water. Consistent with this expectation, the $^{87}Sr/^{86}Sr$ composition of the ocean increased significantly ca. 35.8 Ma (Mead and Hodell, 1995; Zachos et al., 1999) (Figs. 3B and 3F). Increased deposition of kaolinite and chlorite in the Southern Ocean during this same time also suggests an intensification of weathering on Antarctica (Ehrmann and Mackensen, 1992; Zachos et al., 1999). Both of these independent observations support our hypothesis of large-scale glaciation of Antarctica ca. 36.0 Ma and subsequent ice-sheet retreat ca. 35.8 Ma.

Two factors may have contributed to the growth and decay of a large Antarctic Ice Sheet. First, atmospheric CO_2 declined by >1000 ppm through the Eocene and Oligocene (Zachos et al., 2008), but also underwent several oscillations, beginning with a drop to 660–930 ppm ca. 36 Ma (Pagani et al., 2005) (Fig. 3C). Glacial climate model simulations suggest a threshold response of Antarctic glaciation to a drop in CO_2 below ~750 ppm, with ice-sheet growth causing a sea-level fall of 40–50 m and an increase in ocean $\delta^{18}O$ of ~0.30‰ (DeConto and Pollard, 2003; DeConto et al., 2008). These predictions are consistent with the sea-level history recorded by the incised valley fill complex at Wadi Al-Hitan and with benthic $\delta^{18}O$ records (Fig. 3D).

The second factor that may have contributed to the onset of glaciation in Antarctica is a change in Earth's orbital parameters, wherein a reduction in the peak amplitude of austral summer insolation at the onset of the CO_2 decline (Fig. 3E) enhanced the accumulation of snow and ice via diminished summer ablation. Orbital cycles may have been important in promoting the glaciation of Antarctica prior to the major global cooling ca. 33.8 Ma (Liu et al., 2009), but orbital parameters alone cannot explain the onset or termination of glaciation because they are nonunique (Laskar et al., 2004). This leaves change in atmospheric CO_2 as the most probable driver of the transient glaciation and deglaciation of Antarctica during the Late Eocene.

The physical and geochemical evidence presented here indicates that the Antarctic Ice Sheet achieved at least 70% of the volume of the present-day East Antarctic Ice Sheet ca. 36.0 Ma before partially or wholly melting. Growth and decay of the ice sheet appear to have been paced by changes in atmospheric CO_2 concentration that oscillated around ~750 ppm. Furthermore, sea level fluctuated tens of meters during this interval, suggesting a highly volatile East Antarctic Ice Sheet when CO_2 concentrations were near this threshold value. Because many of the carbon emission scenarios for the coming century predict that atmospheric CO_2 will cross this same 750 ppm threshold (Soloman et al., 2007), our results raise the possibility that global climate could rapidly transition to a state not unlike the Late Eocene, when a large, permanent East Antarctic Ice Sheet was not sustainable.

ACKNOWLEDGMENTS

We thank A. Carroll, P. Cohen, B. Wilkinson, and P.I. McLaughlin for discussion and M.S. Antar, E. Williams, and I. Zalmout for help in the field. M.M. Fouda, Director of the Nature Conservation Sector of the Egyptian Environmental Affairs Agency, encouraged work at Wadi Al-Hitan. We also thank B. Wade and two anonymous reviewers for helpful comments. Research supported by the Egyptian Mineral Resources Authority, Cairo Geological Museum, Egyptian Environmental Affairs Agency, and U.S. National Science Foundation (grants 0517773 and 0920972).

REFERENCES CITED

Barker, P.F., Diekmann, B., and Escutia, C., 2007, Onset of Cenozoic Antarctic glaciation: Deep-Sea Research II, v. 54, p. 2293–2307, doi: 10.1016/j.dsr2.2007.07.027.

Berggren, W.A., Kent, D.V., Swisher, C.C., III, and Aubry, M., 1995, A revised Cenozoic geochronology and chronostratigraphy, *in* Berggren, W.A. et al., eds., Geochronology, time scales and global stratigraphic correlation: SEPM (Society for Sedimentary Geology) Special Publication 54, p. 129–212.

Blum, J.D., and Erel, Y., 1995, A silicate weathering mechanism linking increases in marine $^{87}Sr/^{86}Sr$ with global glaciation: Nature, v. 373, p. 415–418, doi: 10.1038/373415a0.

Coxall, H.K., Wilson, P.A., Pälike, H., Lear, C.H., and Backman, J., 2005, Rapid stepwise onset of Antarctic glaciation and deeper calcite compensation in the Pacific Ocean: Nature, v. 433, p. 53–57, doi: 10.1038/nature03135.

DeConto, R.M., and Pollard, D., 2003, Rapid Cenozoic glaciation of Antarctica induced by declining atmospheric CO_2: Nature, v. 421, p. 245–249, doi: 10.1038/nature01290.

DeConto, R.M., Pollard, D., Wilson, P.A., Pälike, H., Lear, C.H., and Pagani, M., 2008, Thresholds for Cenozoic bipolar glaciation: Nature, v. 455, p. 652–656, doi: 10.1038/nature07337.

Ehrmann, W.U., and Mackensen, A., 1992, Sedimentological evidence for the formation of an East Antarctic ice sheet in Eocene/Oligocene time: Palaeogeography, Palaeoclimatology, Palaeoecology, v. 93, p. 85–112, doi: 10.1016/0031-0182(92)90185-8.

Gradstein, F., Ogg, J., and Smith, A., 2004, A geologic time scale 2004: Cambridge, Cambridge University Press, 589 p.

Hardenbol, J., Jacques, T., Martin, F.B., Pierre-Charles, G., and Vail, P.R., 1998, Mesozoic and Cenozoic sequence chronostratigraphy framework of European basins, *in* de Graciansky, PC., et al., eds., Mesozoic and Cenozoic sequence stratigraphy of European Basins: SEPM (Society for Sedimentary Geology) Special Publication 60, p. 3–13.

Huber, M., and Nof, D., 2006, The ocean circulation in the Southern Hemisphere and its climatic impacts in the Eocene: Palaeogeography, Palaeoclimatology, Palaeoecology, v. 231, p. 9–28, doi: 10.1016/j.palaeo.2005.07.037.

Katz, M.E., Miller, K.G., Wright, J.D., Wade, B.S., Browning, J.V., Cramer, B.S., and Rosenthal, Y., 2008, Stepwise transition from the Eocene greenhouse to the Oligocene icehouse: Nature Geoscience, v. 1, p. 329–334, doi: 10.1038/ngeo179.

Kennett, J.P., 1977, Cenozoic evolution of Antarctic glaciation, the circum-Antarctic ocean, and their impact on global palaeoceanography: Journal of Geophysical Research, v. 82, p. 3843–3860, doi: 10.1029/JC082i027p03843.

Laskar, J., Robutel, P., Joutel, F., Gastineau, M., Correia, A.C.M., and Levrard, B., 2004, A long-term numerical solution for the insolation quantities of the Earth: Astronomy & Astrophysics, v. 428, p. 261–285, doi: 10.1051/0004-6361:20041335.

Lear, C.H., Bailey, T.R., Pearson, P.N., Coxall, H.K., and Rosenthal, Y., 2008, Cooling and ice growth across the Eocene-Oligocene transition: Geology, v. 36, p. 251–254, doi: 10.1130/G24584A.1.

Liu, Z., Pagani, M., Zinniker, D., DeConto, R., Huber, M., Brinkhuis, H., Shah, S.R., Leckie, R.M., and Pearson, A., 2009, Global cooling during the Eocene-Oligocene climate transition: Science, v. 323, p. 1187–1190, doi: 10.1126/science.1166368.

Mattheus, C.R., Rodriguez, A.B., Greene, D.L., Simms, A.R., and Anderson, J.B., 2007, Control of upstream variables on incised-valley dimension: Journal of Sedimentary Research, v. 77, p. 213–224, doi: 10.2110/jsr.2007.022.

Mead, G.A., and Hodell, D.A., 1995, Controls on the $^{87}Sr/^{86}Sr$ composition of seawater from the middle Eocene to Oligocene: Hole 689B, Maud Rise, Antarctica: Paleoceanography, v. 10, p. 327–346, doi: 10.1029/94PA03069.

Miller, K.G., Fairbanks, R.G., and Mountain, G.S., 1987, Tertiary oxygen isotope syntheses, sea level history, and continental margin erosion: Paleoceanography, v. 2, p. 1–19, doi: 10.1029/PA002i001p00001.

Miller, K.G., Browning, J.V., Aubry, M.P., Wade, B.S., Katz, M.E., Kulpecz, A.A., and Wright, J.D., 2008, Eocene-Oligocene global climate and sea-level changes: St. Stephens Quarry, Alabama: Geological Society of America Bulletin, v. 120, p. 34–53, doi: 10.1130/B26105.1.

Mitrovica, J.X., Gomez, N., and Clark, P.U., 2009, The sea-level fingerprint of West Antarctic collapse: Science, v. 323, p. 753, doi: 10.1126/science.1166510.

Pagani, M., Zachos, J.C., Freeman, K.H., Tipple, B., and Bohaty, S., 2005, Marked decline in atmospheric carbon dioxide concentrations during the Paleogene: Science, v. 309, p. 600–603, doi: 10.1126/science.1110063.

Pearson, P.N., Foster, G.L., and Wade, B.S., 2009, Atmospheric carbon dioxide through the Eocene-Oligocene climate transition: Nature, v. 461, p. 1110–1113, doi: 10.1038/nature08447.

Perch-Nielsen, K., 1989, Cenozoic calcareous nannofossils, *in* Bolli, H.M., et al., eds., Plankton stratigraphy: Cambridge, Cambridge University Press, p. 427–554.

Peters, S.E., Antar, M.S.M., Zalmout, I.S., and Gingerich, P.D., 2009, Sequence stratigraphic control on preservation of late Eocene whales and other vertebrates at Wadi Al-Hitan, Egypt: Palaios, v. 24, p. 290–302, doi: 10.2110/palo.2008.p08-080r.

Rea, D.K., and Lyle, M.W., 2005, Paleogene calcite compensation depth in the eastern subtropical Pacific; answers and questions: Paleoceanography, v. 20, PA1012, doi: 10.1029/2004PA001064.

Roy, M., van de Flierdt, T., Hemming, S.R., and Goldstein, S.L., 2007, $^{40}Ar/^{39}Ar$ ages of hornblende grains and bulk Sm/Nd isotopes of circum-Antarctic glacio-marine sediments: Implications for sediment provenance in the southern ocean: Chemical Geology, v. 244, p. 507–519, doi: 10.1016/j.chemgeo.2007.07.017.

Salem, R., 1976, Evolution of Eocene-Miocene sedimentation patterns in parts of northern Egypt: American Association of Petroleum Geologists Bulletin, v. 60, p. 34–64.

Soloman, S.D., Manning, M., and Qin, D., 2007, Climate change 2007: The physical science basis: Contribution of Working Group I to the Fourth Assessment Report of the Intergovernmental Panel on Climate Change: Cambridge, Cambridge University Press.

Vonhof, H.B., Smit, J., Brinkhuis, H., Montanari, A., and Nederbragt, A.J., 2000, Global cooling accelerated by early late Eocene impacts?: Geology, v. 28, p. 687–690, doi: 10.1130/0091-7613(2000)28<687:GCABEL>2.0.CO;2.

Watts, A.B., 1982, Tectonic subsidence, flexure and global changes of sea level: Nature, v. 297, p. 469–474, doi: 10.1038/297469a0.

Wilson, G.S., Roberts, A.P., Verosub, K.L., Florindo, F., and Sagnotti, L., 1998, Magnetobiostratigraphic chronology of the Eocene-Oligocene transition in the CIROS-1 core, Victoria Land margin, Antarctica: Implications for Antarctic glacial history: Geological Society of America Bulletin, v. 110, p. 35–47, doi: 10.1130/0016-7606(1998)110<0035:MCOTEO>2.3.CO;2.

Zachos, J.C., Opdyke, B.N., Quinn, T.M., Jones, C.E., and Halliday, A.N., 1999, Early Cenozoic glaciation, Antarctic weathering, and seawater $^{87}Sr/^{86}Sr$: Is there a link?: Chemical Geology, v. 161, p. 165–180, doi: 10.1016/S0009-2541(99)00085-6.

Zachos, J., Pagani, M., Sloan, L., Thomas, E., and Billups, K., 2001, Trends, rhythms, and aberrations in global climate 65 Ma to present: Science, v. 292, p. 686–693, doi: 10.1126/science.1059412.

Zachos, J.C., Dickens, G.R., and Zeebe, R.E., 2008, An early Cenozoic perspective on greenhouse gas warming and carbon-cycle dynamics: Nature, v. 451, p. 279–283, doi: 10.1038/nature06588.

Zaitlin, B.A., Dalrymple, R.W., and Boyd, R., 1994, The stratigraphic organization of incised-valley systems associated with relative sea-level changes, *in* Dalrymple, R.W., et al., eds., Incised-valley systems: Origin and sedimentary sequences: SEPM (Society for Sedimentary Geology) Special Publication 51, p. 45–83.

Manuscript received 28 January 2010
Revised manuscript received 10 March 2010
Manuscript accepted 11 March 2010

Printed in USA